

# First-principles study of CuAlS<sub>2</sub> for p-type transparent conductive materials

Dan Huang<sup>1</sup>, Ren-Yu Tian<sup>2</sup>, Yu-Jun Zhao<sup>2,3</sup>, Jian-Jun Nie<sup>1</sup>, Xin-Hua Cai<sup>1</sup>  
and Chun-Mei Yao<sup>1</sup>

<sup>1</sup> Department of Physics and Electronic Sciences, Hunan University of Arts and Science, Changde, Hunan 415000, People's Republic of China

<sup>2</sup> Department of Physics, South China University of Technology, Guangzhou, Guangdong 510640, People's Republic of China

E-mail: zhaoyj@scut.edu.cn

Received 17 July 2010, in final form 17 August 2010

Published 16 September 2010

Online at [stacks.iop.org/JPhysD/43/395405](http://stacks.iop.org/JPhysD/43/395405)

## Abstract

We have investigated the intrinsic defects, and Mg, Zn impurities in CuAlS<sub>2</sub>, as well as their induced carrier concentrations using the first-principles calculations. We find that p-type conductivity could be dominated by the intrinsic defects V<sub>Cu</sub>, Cu<sub>Al</sub> or the doping defects Zn<sub>Al</sub>, Mg<sub>Al</sub> in different samples. Although vacancy Cu is an important acceptor in CuAlS<sub>2</sub>, a Cu-deficient sample is not the best for p-type conductivity due to the compensation from Al<sub>Cu</sub> defects. In fact, our results indicate that Zn is the best choice for p-type doping for CuAlS<sub>2</sub>, in particular under Cu-rich and Al-poor condition, which is in line with the experimental results. The main difference in carrier concentration between theory and experiment is expected to have originated from the multiphase of the samples prepared in experiments, instead of a single crystal. We also find that there is no remarkable difference in the effective mass in samples dominated by different defects, such as Cu<sub>Al</sub>, Mg<sub>Al</sub>, Zn<sub>Al</sub> and Cu vacancy. The significant difference in the experimentally observed hole mobility may be dominated by their mean free time  $\tau_p$ .

(Some figures in this article are in colour only in the electronic version)

## 1. Introduction

Materials with transparency of glasses and conductivity of metals have attracted considerable interest for novel information and energy devices, such as transparent electrodes in solar cells, low emissivity windows and information displays. These materials are called transparent conductive materials (TCMs), requiring carrier concentrations of at least  $10^{20} \text{ cm}^{-3}$  and optical band gaps greater than 3 eV [1]. Development of functional p–n junctions solely using TCMs is a vital goal for material scientists, because it is expected to open up an era of ‘transparent electronics’ [2]. Established TCMs, such as Sn-doped In<sub>2</sub>O<sub>3</sub> [3], F-doped SnO<sub>2</sub> [4] and Al-doped ZnO [5] are all n-type materials intrinsically. The p-type doping with good performance for these materials looks pessimistic in spite of a flurry of attempts, which has clearly limited their practical applications. Therefore, it is crucial

to find an excellent p-type TCM for a possible transparent electronic era.

Since CuAlO<sub>2</sub> was reported to possess a conductivity of  $1.0 \text{ S cm}^{-1}$  at room temperature in 1997 [6], p-type metal oxides have been attracting considerable attention for p-type TCMs. Almost all copper oxide-based delafossite structure semiconductors are p-type TCMs, such as CuAlO<sub>2</sub> [6], CuGaO<sub>2</sub> [7], CuInO<sub>2</sub> [8], CuScO<sub>2</sub> [9] and CuYO<sub>2</sub> [10], but their conductivities are  $10^3$ – $10^4$  times lower than that of well established n-type transparent conducting oxides (TCOs) for the hole localization of anion oxides. Nie *et al* [11] have revealed that this delafossite family does not exhibit direct band gap by first-principles study. On the other hand, sulfides have been found to be promising candidates. For example, high hole mobility and electrical conductivity were reported in p-type doped BaCu<sub>2</sub>S<sub>2</sub> [12], although its band gap (2.3 eV) is too narrow for practical TCM applications.

<sup>3</sup> Author to whom any correspondence should be addressed.

Recently, significant promotion of high p-type conductivity at room temperature has been reported in a series of nonstoichiometry of Zn/Mg-doped CuAlS<sub>2</sub> [13–17]. For example, CuAl<sub>0.9</sub>Zn<sub>0.1</sub>S<sub>2</sub> [13] has shown a conductivity of up to 63.5 S cm<sup>-1</sup> and the average transmittance in the visible region is above 80%. In addition, CuAlS<sub>2</sub> has other unique properties in favour of microelectronic applications. It has a chalcopyrite structure and is expected to integrate easily with conventional semiconductors of zinc-blende structures. It possesses a wide direct band gap of about 3.49 eV, which satisfies the band gap requirement for TCMs [18]. Its exciton binding energy (70 meV) [19] is greater than that of most other ultraviolet emitting materials such as ZnO (60 meV), ZnS (39 meV) and GaN (21 meV) [20]. Although there are many research efforts on the electrical properties of CuAlS<sub>2</sub> from experiment, the microscopic origin of p-type conductivity is still unclear. This may hinder the improvement on the stability of its remarkable p-type properties.

In this work, we study the defect properties and their related conductivity properties in CuAlS<sub>2</sub> using the first-principles method. Our results indicate that Zn is the best choice for the p-type doping of CuAlS<sub>2</sub>, in particular under Cu-rich and Al-poor condition, which is consistent with the experimental results [13]. Decreasing Cu content ratio in CuAlS<sub>2</sub> (i.e. Cu<sub>1-x</sub>AlS<sub>2</sub>  $x > 0$ ) to increase Cu vacancy concentration will be accompanied by an increase in donor defect Al<sub>Cu</sub>, which impedes the increase in p-type carrier concentration. On the other hand, CuAlS<sub>2+x</sub>, Cu<sub>1+x</sub>Al<sub>1-x</sub>S<sub>2</sub>, CuAl<sub>1-x</sub>Zn<sub>x</sub>S<sub>2</sub> and CuAl<sub>1-x</sub>Mg<sub>x</sub>S<sub>2</sub> ( $x > 0$ ) could have higher p-type carrier concentration owing to no remarkable compensating donor defects. Combining the data of defect formation enthalpies and overall charge neutrality of all the studied charged defects, we have calculated the carrier concentration in various samples under different conditions, which is remarkably smaller than the experimental values at room temperature. The difference between the experimental observation and our calculated results is expected to have originated from the multiphase in the experimental samples.

The difference in hole mobility among the samples dominated by substituting defects (Cu<sub>Al</sub>, Mg<sub>Al</sub>, Zn<sub>Al</sub>) and Cu vacancies should be attributed mainly to the mean free time  $\tau_p$ , since their effective mass shows no significant difference.

## 2. Computational details

Our first-principles calculations are carried out within the density functional theory (DFT) and the PW91 GGA formalism [21] for the exchange and correlation functionals. A plane-wave basis set and projector augmented wave potentials [22] are employed as implemented in the Vienna Ab-initio Simulation Package (VASP) [23, 24]. An energy cutoff of 500 eV is used throughout the calculations. Brillouin zone integrations are performed with the special  $k$ -point scheme over a  $3 \times 3 \times 3$  Monkhorst–Pack mesh for a supercell consisting of  $2 \times 2 \times 1$  unit cells (64 atoms). The theoretically calculated equilibrium lattice parameters of CuAlS<sub>2</sub>,  $a = 5.341 \text{ \AA}$ ,  $c = 10.513 \text{ \AA}$ , are employed, and the internal coordinates are fully relaxed throughout this work.

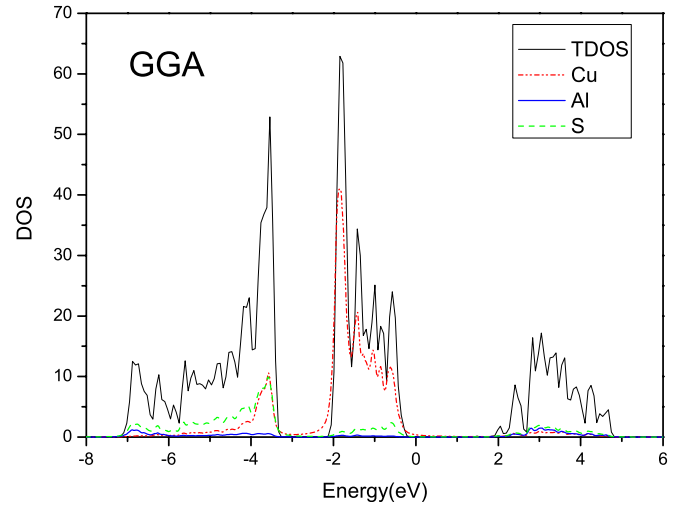


Figure 1. The DOS of CuAlS<sub>2</sub>. (Colour online.)

## 3. Intrinsic defects in CuAlS<sub>2</sub> and induced carrier concentration

CuAlS<sub>2</sub> has a chalcopyrite structure (space group number: 122), which is analogous to the zinc-blende structure with its cations substituted by two types of cations alternately along the  $\langle 001 \rangle$  direction. Our calculated lattice parameters of CuAlS<sub>2</sub> are  $a = 5.341 \text{ \AA}$ ,  $c = 10.513 \text{ \AA}$ , which are in good agreement with experimental measurements,  $a = 5.334 \text{ \AA}$ ,  $c = 10.444 \text{ \AA}$  [25], within an error of 0.7%.

Figure 1 shows the density of states (DOS) of CuAlS<sub>2</sub>. The majority of the lower valence bands ( $-7$  to  $-3$  eV w.r.t. the Fermi level) are dominated by Cu and S, and the majority of the upper valence bands ( $-2$  to  $0$  eV) are dominated by Cu with a noticeable contribution from S. According to Raebiger *et al* [26], the valence band maximum (VBM) should be formed by the interaction between a filled anion shell and a filled cation shell that lie as high in energy as possible for an expected p-type material. The p-type doping of a semiconductor is facilitated by the repulsive interaction between the p orbitals of atomic anions and filled d-shell states of metal cations that have a higher energy compared with the anion p orbitals' atomic level [26]. If the VBM were formed by the bonding state and with the character of the anion p state, the VBM would stay at a low energy state. Then, the hole near the VBM with the anion dangling bond character would be localized, which is harmful for p-type conductivity. The VBM of CuAlS<sub>2</sub> is formed by the anti-bonding state between Cu and S and far from the majority of the anion p states, which follows the general rule for p-type material design. This indicates that CuAlS<sub>2</sub> is expected to be a good candidate for p-type conductive materials.

The formation enthalpies for the intrinsic and extrinsic defects are calculated in a  $2 \times 2 \times 1$  CuAlS<sub>2</sub> supercell consisting of 64 atoms according to [27]:

$$\Delta H(D, q) = E(D, q) - E(0) + \sum_{\alpha} n_{\alpha} (\Delta \mu_{\alpha} + \mu_{\alpha}^{\text{solid}}) + q(E_{\text{VBM}} + E_{\text{F}}), \quad (1)$$

where  $E(D, q)$  and  $E(0)$  are the total energy of the supercells with and without a defect. Here  $(\Delta \mu_{\alpha} + \mu_{\alpha}^{\text{solid}})$  is the absolute

value of the chemical potential of atom  $\alpha$ .  $\mu_\alpha^{\text{solid}}$  is defined as the chemical potential of the elemental solid. Also  $n_\alpha$  is the number of atoms for each defect;  $n_\alpha = -1$  if an atom is added, while  $n_\alpha = 1$  if an atom is removed.  $E_{\text{VBM}}$  represents the energy of the VBM of the defect-free system and  $E_F$  is the Fermi energy relative to the  $E_{\text{VBM}}$ . For charged systems, a compensating homogeneous jellium background charge is assumed to preserve overall neutrality. Recently, Lany and Zunger [28] have found that the formation energy of GaAs:  $\text{V}_{\text{As}}^{3+}$  could be well converged in fairly small supercells such as a 64-atom or even a 32-atom supercell, as long as the potential alignment and image charge correction are included. Considering the 64-atom supercells adopted in this work, we have carried out the calculations with both potential alignment and image charge correction. The potential alignment is considered by adding  $\Delta V$  into the  $(E_{\text{VBM}} + E_F)$  term, where  $\Delta V$  is the electrostatic alignment between the doped host and the pure host. For the image charge correction, the Makov–Payne correction [29] (including the quadrupole term) is employed.

The chemical potentials of each constituent species ( $\Delta\mu_\alpha$ ) can be varied to reflect specific equilibrium growth conditions, but their summation is always equal to the calculated formation enthalpy of  $\text{CuAlS}_2$  in order to maintain the stability of the host:

$$\Delta\mu_{\text{Cu}} + \Delta\mu_{\text{Al}} + 2\Delta\mu_{\text{S}} = \Delta H(\text{CuAlS}_2) = -3.43 \text{ eV}. \quad (2)$$

In addition to the host stability condition, the atomic chemical potentials should be smaller than that of the corresponding elemental solid to avoid precipitation of elemental solids:

$$\Delta\mu_{\text{Cu}} \leq 0, \quad \Delta\mu_{\text{Al}} \leq 0, \quad \Delta\mu_{\text{S}} \leq 0. \quad (3)$$

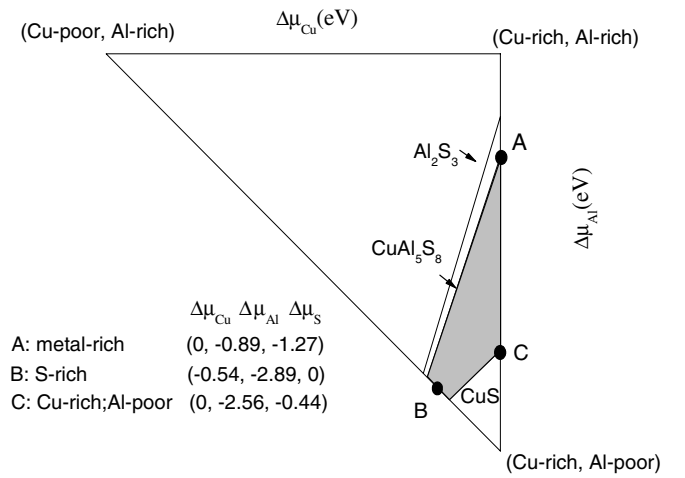
The chemical potentials are further restricted by the competing compounds. According to our previous works [30], the main competing phases are  $\text{Al}_2\text{S}_3$  and  $\text{CuS}$ . Here we considered an additional ternary competing phase,  $\text{CuAl}_5\text{S}_8$ . These crucial constraints are listed as follows:

$$2\Delta\mu_{\text{Al}} + 3\Delta\mu_{\text{S}} \leq \Delta H(\text{Al}_2\text{S}_3) = -5.52 \text{ eV}, \quad (4)$$

$$\Delta\mu_{\text{Cu}} + \Delta\mu_{\text{S}} \leq \Delta H(\text{CuS}) = -0.44 \text{ eV}, \quad (5)$$

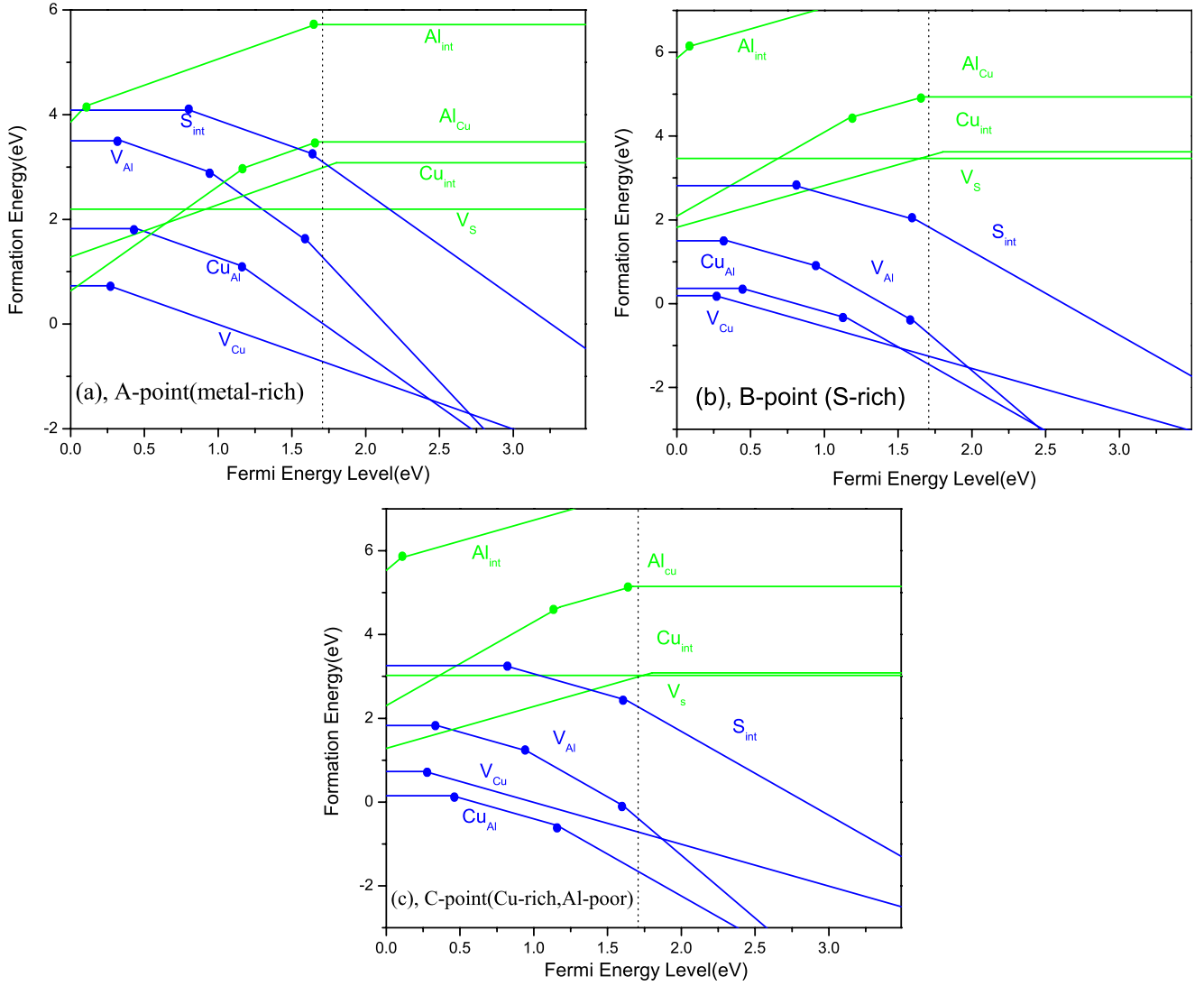
$$\Delta\mu_{\text{Cu}} + 5\Delta\mu_{\text{Al}} + 8\Delta\mu_{\text{S}} \leq \Delta H(\text{CuAl}_5\text{S}_8) = -14.61 \text{ eV}. \quad (6)$$

Figure 2 shows the calculated chemical potential domains for  $\text{CuAlS}_2$ . From the constraints imposed by the competing compounds, the shaded grey areas are the allowed chemical potential ranges for  $\text{CuAlS}_2$ . Within this boundary, we explicitly consider three extreme growth conditions. The first one is metal-rich condition (point A in figure 2), where the chemical potential  $\Delta\mu_\alpha$  reaches a maximum for Cu and Al. The second one is S-rich condition (point B in figure 2), where the chemical potential  $\Delta\mu_{\text{S}}$  reaches a maximum (0 eV). The last one is Cu-rich and Al-poor condition (point C in figure 2), where  $\Delta\mu_{\text{Cu}}$  reaches a maximum and  $\Delta\mu_{\text{Al}}$  is relatively low. The detailed values of the chemical potentials of Cu, Al and S under different growth conditions are shown in figure 2.



**Figure 2.** The chemical potential ranges for a stable  $\text{CuAlS}_2$ . The grey areas are the allowed chemical potential range for  $\text{CuAlS}_2$  with consideration of competing compounds. Points A, B and C represent three extreme conditions considered in this work.

Figure 3 shows the formation enthalpy of intrinsic defects in  $\text{CuAlS}_2$  under different conditions with the potential alignment and image charge correction. Common defects such as vacancies, interstitial and antisite defects are considered here. Obviously, acceptor defects (mainly  $\text{V}_{\text{Cu}}$  and  $\text{Cu}_{\text{Al}}$ ) have the lowest formation enthalpy under various extreme conditions except that  $\text{Al}_{\text{Cu}}$  defect dominates near the VBM under metal-rich condition (cf figure 3(a)). The p-type conductivity should have originated mainly from  $\text{V}_{\text{Cu}}$  and  $\text{Cu}_{\text{Al}}$ . The defect formation enthalpies have the same trend in energy magnitude but different in transition level with and without the potential alignment and image charge correction. The calculated transition levels of  $\text{V}_{\text{Cu}}$  and  $\text{Cu}_{\text{Al}}$  are 0.26 eV and 0.44 eV, respectively, with the potential alignment and image charge correction. Without these corrections, we find that the transition levels of  $\text{V}_{\text{Cu}}$ ,  $\text{Cu}_{\text{Al}}$  and  $\text{V}_{\text{Al}}$  would be below the VBM, which is unphysical [31]. This indicates the necessity of potential alignment and image charge correction for the calculation of shallow levels, consistent with Lany and Zunger’s work [28], in which they urged the employment of these corrections for the defect formation enthalpy. Like other chalcopyrite semiconductors, Cu vacancy is one of the main defects in  $\text{CuAlS}_2$ . When the Fermi level is close to the VBM, Cu vacancy has the lowest formation enthalpy among the acceptor defects under metal-rich and S-rich conditions (points A and B). Under Cu-rich and Al-poor condition (point C), the  $\text{Cu}_{\text{Al}}$  defect has a lower formation enthalpy than that of  $\text{V}_{\text{Cu}}$ . Under metal-rich condition (point A),  $\text{Al}_{\text{Cu}}$  has a low formation enthalpy and compensates the p-type defects remarkably when the Fermi energy level is near the VBM. This is consistent with the experimental observation that it is hard to have large carrier concentrations in the  $\text{Cu}_{1-x}\text{AlS}_2$  ( $x > 0$ ) samples [14]. When the chemical potential of Al is high (Al-rich), Al would substitute on Cu sites and compensate the hole concentration. In addition, our results are in line with the experimental observation of large carrier concentrations in  $\text{CuAlS}_{2+x}$  ( $x > 0$ ) and  $\text{Cu}_{1+x}\text{Al}_{1-x}\text{S}_2$  ( $x > 0$ ) [15, 16].



**Figure 3.** The formation enthalpy of intrinsic defects in  $\text{CuAlS}_2$  under different conditions with the potential alignment and image charge correction. Red and blue lines represent the donor and acceptor defects, respectively. Here the experimental gap of  $\text{CuAlS}_2$ ,  $E_g = 3.49$  eV, is adopted. (Colour online.)

According to equation (1), the formation energies of various defects depend on the Fermi level of the system, which is in turn balanced by the charges from the various defects, with their concentrations calculated from the corresponding formation energies according to Boltzmann distribution, and the corresponding carrier concentration. Thus, self-consistent calculations are required for defect concentrations, Fermi level and carrier concentrations at room temperature and growth temperature based on the charge neutrality of the system [32,33]. In the concentration calculation of this work,  $T = 773$  K of substrate temperature is adopted for the growth temperature [13]. Under room temperature, the p-type carrier concentration is calculated to be  $8.16 \times 10^{16} \text{ cm}^{-3}$ ,  $1.90 \times 10^{18} \text{ cm}^{-3}$  and  $7.69 \times 10^{16} \text{ cm}^{-3}$  under metal-rich (point A), S-rich (point B) and Cu-rich, Al-poor (point C) conditions, respectively. The defect concentrations clearly indicate that the origin of p-type carrier is the Cu vacancy for both points A and B, but Cu-site Al compensates partial hole concentration at point A, which results in a relatively low carrier concentration

at point A. Owing to the deeper transition level of  $\text{Cu}_{\text{Al}}$ , the carrier concentration at point C is relatively low at room temperature. The p-type carrier can reach  $7.94 \times 10^{19} \text{ cm}^{-3}$  and  $2.67 \times 10^{19} \text{ cm}^{-3}$  at the growth temperature at points B and C, respectively, where no significant hole killers exist. This basically meets the experimental observation except the sharp contrast on the high carrier concentration measured in  $\text{Cu}_{1.08}\text{Al}_{0.92}\text{S}_2$  and low theoretical carrier concentration at point C at room temperature (cf table 1).  $\text{CuAlS}_2$  is known to be intrinsically Cu-deficient, and thus the difference is likely attributed to the fact that multiphase samples are measured in the experiment while a single crystal is adopted in our calculations. In fact, the self-consistent calculated  $E_F$  is nearly located at the VBM at room temperature at points B and C since there are no remarkable compensating n-type defects competing with vacancy Cu or  $\text{Cu}_{\text{Al}}$  acceptor defects. This results in the relative high hole concentration at points B and C.

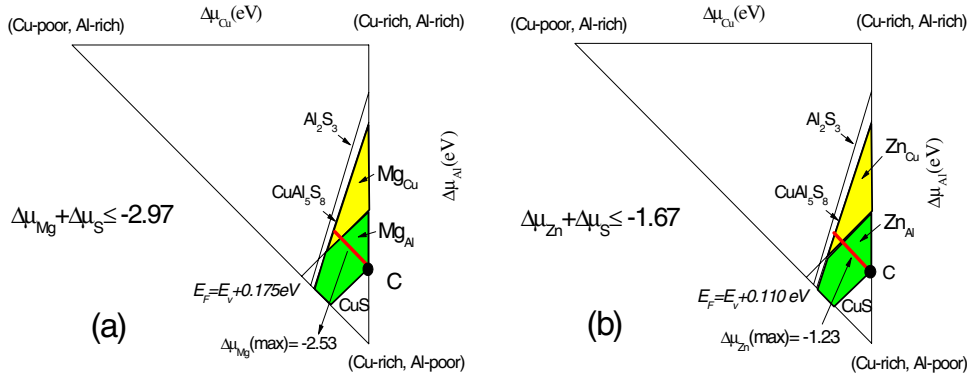


**Figure 4.** The chemical potential range for site preference on Cu or Al of the dopant atoms Mg and Zn (assuming  $E_F = 0.110$  eV for Zn doping and  $E_F = 0.175$  eV for Mg doping above the VBM). The yellow area favours Cu site, while the green area favours Al site for the dopants. (Colour online.)

#### 4. Mg- or Zn-doped CuAlS<sub>2</sub> and its carrier concentration

In this section, we discuss Mg or Zn doping in CuAlS<sub>2</sub> and their impact on the concentration of p-type carriers. First, we will investigate the site preference of Mg and Zn at Cu or Al sites. The site preference is crucial to the electronic property of the sample since Mg and Zn are expected to be donors at Cu sites, but acceptors at Al sites. Their favourable doping site can be determined by their defect formation enthalpies, which depend on the growth conditions.

Although Mg or Zn could be doped at Cu sites as donors, it is hard to change CuAlS<sub>2</sub> as a hole conductor due to the low formation enthalpies of the p-type intrinsic defects such as  $V_{Cu}$ ,  $Cu_{Al}$  and  $V_{Al}$ . Obviously, for a maximum contribution of Mg acceptors, Cu-rich and Al-poor condition (choose point C) is the optimal growth condition. When Mg or Zn is introduced into the CuAlS<sub>2</sub> systems, the chemical domain of CuAlS<sub>2</sub> may be further limited due to the competing phases of MgS or ZnS, with constraints of

$$\Delta\mu_{Mg} + \Delta\mu_S \leq \Delta H(MgS) = -2.97 \text{ eV}, \quad (7)$$

$$\Delta\mu_{Zn} + \Delta\mu_S \leq \Delta H(ZnS) = -1.67 \text{ eV}. \quad (8)$$

Since  $\Delta H(MgS)$  and  $\Delta H(ZnS)$  are constants, the maximum allowed chemical potential for Mg or Zn directly depends on  $\Delta\mu_S$ .

Figure 4 shows the possible Mg (or Zn) site preference at different  $\Delta\mu_{Cu}$ ,  $\Delta\mu_{Al}$  regions, assuming Fermi energy level at 0.175 eV for Mg doping and 0.110 eV for Zn doping, which are obtained from self-consistent calculations at the growth temperature under Cu-rich and Al-poor condition (cf point C in figure 2). Under this condition, substitution of Mg (or Zn) at Al sites will be maximized as the Cu sites are minimized. At point C, the maximum allowed value of  $\Delta\mu_{Mg}$  is  $-2.53$  eV (red line in figure 4(a)). If the value of  $\Delta\mu_{Mg}$  increases, the red line would move up and the green areas for  $Mg_{Al}$  would decrease. For Zn-doped CuAlS<sub>2</sub>, the maximum allowed value of  $\Delta\mu_{Zn}$  allowed for  $Zn_{Al}$  is  $-1.23$  eV at point C (red line in figure 4(b)).

This indicates that Mg prefers the Al site (green area) under Cu-rich and Al-poor condition, whereas Mg prefers Cu

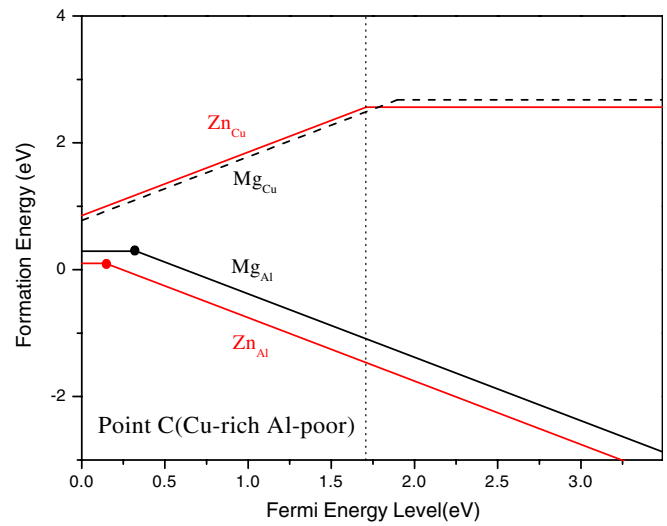


**Figure 5.** The formation enthalpies of Mg ( $\Delta\mu_{Mg} = -2.53$  eV) and Zn ( $\Delta\mu_{Zn} = -1.23$  eV) doped in CuAlS<sub>2</sub> under Cu-rich and Al-poor condition (point C in figure 4). Solid lines and dashed lines represent the acceptor and donor defects, respectively. Here the experimental gap of CuAlS<sub>2</sub>,  $E_g = 3.49$  eV, is adopted. (Colour online.)

site (yellow area) under Al-rich condition. If the Fermi energy level moves towards the conduction band minimum (CBM), the area for  $Mg_{Al}$  or  $Zn_{Al}$  preference in the  $(\Delta\mu_{Cu}, \Delta\mu_{Al})$  plane would increase. A balance point for the Fermi level must exist since  $Mg_{Al}$  or  $Zn_{Al}$  are acceptors, which would impede the Fermi energy level moving to the CBM.

Figure 5 shows the formation enthalpy of Mg ( $\Delta\mu_{Mg} = -2.53$  eV) and Zn ( $\Delta\mu_{Zn} = -1.23$  eV) doped in CuAlS<sub>2</sub> under Cu-rich and Al-poor condition (cf point C in figure 4). The formation enthalpies of  $Mg_{Al}$  and  $Zn_{Al}$  are very low under Cu-rich and Al-poor condition. The transition levels are 0.33 eV and 0.14 eV for  $Mg_{Al}$  and  $Zn_{Al}$ . Our results indicate that Zn doping is better than Mg doping for p-type conductivity. The room temperature p-type carrier concentrations are  $2.53 \times 10^{17} \text{ cm}^{-3}$  and  $3.30 \times 10^{19} \text{ cm}^{-3}$  for Mg-doped and Zn-doped CuAlS<sub>2</sub> from our self-consistent calculation at point C, with significant contribution from  $Mg_{Al}$  or  $Zn_{Al}$ , respectively. Both the defect formation enthalpy and defect concentration indicate that Mg or Zn could dope at Al site easily under certain

**Table 1.** The experimental data of p-type conductivity in some nonstoichiometry or doped CuAlS<sub>2</sub> samples. The dominating defects at room temperature in different samples are suggested according to our calculations, with the main compensating donor defects listed in parentheses as well.

	Experimental			Ref.	Theoretical		Calculated carrier concentration, $p$ (cm <sup>-3</sup> )
	Carrier concentration, $p$ (10 <sup>19</sup> cm <sup>-3</sup> )	Hole mobility, $\mu_p$ (cm <sup>2</sup> V <sup>-1</sup> s <sup>-1</sup> )	Electric conductivity, $\sigma$ (S cm <sup>-1</sup> )		Dominating defects	Corresponding condition	
Cu <sub>0.98</sub> AlS <sub>2</sub>	0.89	0.3	0.4	14	V <sub>Cu</sub>	Metal-rich (A point in figure 2)	8.16 × 10 <sup>16</sup>
Cu <sub>0.92</sub> AlS <sub>2</sub>	1.68	0.02	0.05		V <sub>Cu</sub> (Al <sub>Cu</sub> )		
CuAlS <sub>2.1</sub>	6.9	0.41	4.6	15	V <sub>Cu</sub> and Cu <sub>Al</sub>	S-rich (B point in figure 2)	1.90 × 10 <sup>18</sup>
Cu <sub>1.08</sub> Al <sub>0.92</sub> S <sub>2</sub>	7.3	21.2	247.5	16	Cu <sub>Al</sub> and V <sub>Cu</sub>	Cu-rich and Al-poor (C point in figure 2)	7.69 × 10 <sup>16</sup>
CuAl <sub>0.9</sub> Zn <sub>0.1</sub> S <sub>2</sub>	6.9	5.7	65.3	13	Zn <sub>Al</sub>	$\Delta\mu_{Zn}$ (max) at C point	3.30 × 10 <sup>19</sup>
CuAl <sub>0.94</sub> Mg <sub>0.06</sub> S <sub>2</sub>	5.6	4.6	41.7	17	Mg <sub>Al</sub>	$\Delta\mu_{Mg}$ (max) at C point	2.53 × 10 <sup>17</sup>

condition, in line with the high doping concentration of Zn or Mg in experimental reports [13, 17].

The experimental results of p-type conductivity in nonstoichiometry or doped CuAlS<sub>2</sub> samples, as well as the suggested dominating defects from our calculations, are listed in table 1. The final electrical conductivity origins from not only carrier concentration but also their hole mobility. The electrical conductivity for a p-type semiconductor satisfies [34]

$$\sigma = pq\mu_p, \quad (9)$$

where  $\sigma$ ,  $p$ ,  $q$  and  $\mu_p$  stand for the electronic conductivity, hole concentration, electronic charge and hole mobility, respectively.

From table 1, we find that the carrier concentration depends on the doping concentration, which is related to the vacancy concentration. We find that the slight increase in carrier concentration in Cu<sub>0.92</sub>AlS<sub>2</sub> compared with Cu<sub>0.98</sub>AlS<sub>2</sub> is affected mainly by the compensated donor defect Al<sub>Cu</sub>. Our earlier discussions have indicated that there are no remarkable compensated donor defects in other listed samples in table 1, which could reach a relatively higher hole concentration.

Based on the above discussion, we can conclude that the hole mobility in the Cu-vacancy dominated samples is much smaller than that in the substituting defect dominated samples. It is known that the hole mobility is decided by the effective mass  $m^*$  and the mean free time  $\tau_p$  [34]:

$$\mu_p = \frac{q\tau_p}{m^*}. \quad (10)$$

The effective mass  $m^*$  could be calculated by the first-principles calculation, but the mean free time  $\tau_p$  is hard to handle. Table 2 lists our calculated effective mass  $m^*$  of holes in the samples with different kinds of defects. We find that the hole mobility  $\mu_p$  of the samples increases as the effective mass  $m^*$  decreases. However, the hole mobility changes by

**Table 2.** The effective mass of the defects in different directions. The calculation is performed in a 16-atom cell. Results from 64-atom supercell calculation are listed in brackets for comparison (unit:  $m_0$ ).

	Gamma-X	Gamma-T	Gamma-N
V <sub>Cu</sub>	-3.27 (-2.90)	-0.90	-2.65
Mg <sub>Al</sub>	-2.92 (-2.77)	-0.79	-2.48
Zn <sub>Al</sub>	-2.43 (-2.66)	-0.69	-2.17
Cu <sub>Al</sub>	-2.19 (-2.60)	-0.67	-1.97

several orders of magnitude, while the effective mass  $m^*$  is in the same order. Obviously, the mean free time  $\tau_p$  plays a crucial role in the hole mobility. Meanwhile, it is noted that the hole mobility in the Cu-vacancy dominated sample is much smaller than that in the samples dominated by the substituting defects, particularly for Cu<sub>Al</sub>. Thus, we expect that the p-type substituting defect will provide a better p-type conductivity in CuAlS<sub>2</sub>.

## 5. Conclusion

In summary, we have investigated the intrinsic and extrinsic defects as well as their influence on the p-type conductivity in CuAlS<sub>2</sub>. We demonstrate that the p-type conductivity origins from V<sub>Cu</sub>, Cu<sub>Al</sub> (Mg<sub>Al</sub>, Zn<sub>Al</sub>) in different samples. Our results show that potential alignment and image charge correction should be employed for the defect formation enthalpy calculation when shallow levels are handled with finite supercells. The Zn<sub>Al</sub> defect has the shallowest acceptor level of 0.14 eV, which is consistent with the best reported results from the experiment. The slight increase in carrier concentration is attributed to the compensated donor defects Al<sub>Cu</sub> in Cu<sub>0.92</sub>AlS<sub>2</sub>. However, CuAlS<sub>2+x</sub>, Cu<sub>1+x</sub>Al<sub>1-x</sub>S<sub>2</sub>, CuAl<sub>1-x</sub>Zn<sub>x</sub>S<sub>2</sub> and CuAl<sub>1-x</sub>Mg<sub>x</sub>S<sub>2</sub> ( $x > 0$ ) could have higher p-type carrier concentration due to the absence of

compensated donor defects. The smaller carrier concentration from calculations could have originated from the multiphase of the samples prepared in the experiments, instead of the ideal crystal used in modelling. As the difference in the effective mass is negligible between the carriers originated from the substituting Mg or Zn defects and Cu vacancies, the remarkable difference in their hole mobility would be dominated by their mean free time  $\tau_p$ .

### Acknowledgments

This work was financially supported by the National Natural Science Foundation of China (NSFC) under Grant No 10704025, the Fundamental Research Funds for the Central Universities, SCUT, under projects 2009ZZ0068 and 2009ZM0165, and the 11th Five-year Plan for Key Construction Academic Subject (Optics) of Hunan Province. The authors acknowledge the computer time at the High Performance Computer Center of the Shenzhen Institute of Advanced Technology (SIAT), the Chinese Academy of Science.

### References

- [1] Gordon R G 2000 *MRS Bull.* **25** 52
- [2] Thomas G 1997 *Nature* **389** 907
- [3] Harvey S P et al 2006 *J. Phys. D: Appl. Phys.* **39** 3959
- [4] Remes Z et al 2009 *Thin Solid Films* **517** 6287
- [5] Wu K et al 2007 *Nanotechnology* **18** 305604
- [6] Kawazoe H et al 1997 *Nature* **389** 939
- [7] Pellicer-Porres J et al 2004 *Phys. Rev. B* **69** 024109
- [8] Yanagi H et al 2001 *Appl. Phys. Lett.* **78** 1583
- [9] Duan N et al 2000 *Appl. Phys. Lett.* **77** 1325
- [10] Jayaraj M K et al 2001 *Thin Solid Films* **397** 244
- [11] Nie X L, Wei S H and Zhang S B 2002 *Phys. Rev. Lett.* **88** 066405
- [12] Park S et al 2002 *Appl. Phys. Lett.* **80** 4393
- [13] Liu M L et al 2007 *Appl. Phys. Lett.* **90** 072109
- [14] Liu M L et al 2008 *Key Eng. Mater.* **368–372** 666
- [15] Liu M L et al 2008 *Scr. Mater.* **58** 1002
- [16] Huang F Q et al 2006 *China Patent* No 200610025073.1
- [17] Liu M L et al 2007 *Scr. Mater.* **57** 1133
- [18] Brini R et al 2009 *Thin Solid Films* **517** 2191
- [19] Chichibu S et al 1997 *Japan. J. Appl. Phys. Part 1* **36** 1703
- [20] Chen Y et al 1998 *J. Appl. Phys.* **84** 3912
- [21] Perdew J P and Wang Y 1992 *Phys. Rev. B* **45** 13244
- [22] Kresse G and Joubert J 1999 *Phys. Rev. B* **59** 1758
- [23] Kresse G and Hafner J 1993 *Phys. Rev. B* **47** R558
- [24] Kresse G and Furthmüller J 1996 *Phys. Rev. B* **54** 11169
- [25] Brandt G et al 1973 *Solid State Commun.* **12** 481
- [26] Raebiger H et al 2007 *Phys. Rev. B* **76** 045209
- [27] Zhang S B et al 2001 *Phys. Rev. B* **63** 075205
- [28] Lany S and Zunger A 2008 *Phys. Rev. B* **78** 235104
- [29] Makov G and Payne M C 1995 *Phys. Rev. B* **51** 4014
- [30] Zhao Y J and Zunger A 2004 *Phys. Rev. B* **69** 075208
- [31] Du M H and Zhang S B 2009 *Phys. Rev. B* **80** 115217
- [32] Persson C et al 2005 *Phys. Rev. B* **72** 035211
- [33] Zhao Y J et al 2004 *Appl. Phys. Lett.* **85** 5860
- [34] Liu E K et al 2007 *Semiconductor Physics* 6th edn (Beijing: Electronic Industry Press) (in Chinese)